Oxidized dNTPs and the OGG1 and MUTYH DNA glycosylases combine to induce CAG/CTG repeat instability

Piera Cilli[1,2], Ilenia Ventura[1], Anna Minoprio[1], Ettore Meccia[1], Alberto Martire[3], Samuel H. Wilson[4], Margherita Bignami[1,*] and Filomena Mazzei[1,*]

[1]Department of Environment and Primary Prevention, Istituto Superiore di Sanità, 00161 Roma, Italy, [2]Department of Science, University Roma Tre, 00154 Roma, Italy, [3]Department of Drug Safety and Evaluation, Istituto Superiore di Sanità, 00161 Roma, Italy and [4]Genome Integrity and Structural Biology Laboratory, National Institute of Environmental Health Sciences, National Institutes of Health, Research Triangle Park, NC 27709, USA

ABSTRACT

DNA trinucleotide repeat (TNR) expansion underlies several neurodegenerative disorders including Huntington's disease (HD). Accumulation of oxidized DNA bases and their inefficient processing by base excision repair (BER) are among the factors suggested to contribute to TNR expansion. In this study, we have examined whether oxidation of the purine dNTPs in the dNTP pool provides a source of DNA damage that promotes TNR expansion. We demonstrate that during BER of 8-oxoguanine (8-oxodG) in TNR sequences, DNA polymerase β (POL β) can incorporate 8-oxodGMP with the formation of 8-oxodG:C and 8-oxodG:A mispairs. Their processing by the OGG1 and MUTYH DNA glycosylases generates closely spaced incisions on opposite DNA strands that are permissive for TNR expansion. Evidence in HD model R6/2 mice indicates that these DNA glycosylases are present in brain areas affected by neurodegeneration. Consistent with prevailing oxidative stress, the same brain areas contained increased DNA 8-oxodG levels and expression of the p53-inducible ribonucleotide reductase. Our *in vitro* and *in vivo* data support a model where an oxidized dNTPs pool together with aberrant BER processing contribute to TNR expansion in non-replicating cells.

INTRODUCTION

Oxidative stress is considered a risk factor in several neurodegenerative diseases. Huntington's disease (HD) is a progressive neurodegenerative disorder caused by expansion of CAG repeats in the *huntingtin (HTT)* gene, with the length of the repeats being the main determinant of the age of onset (1–2). In HD patients and in mouse models, expression of mutant HTT (expanded allele sizes ranging CAG 35–121) is associated with increased formation of reactive oxygen species (ROS) and accumulation of oxidative damage to DNA, proteins and lipids. Thus post-mortem brains of HD patients contain higher than normal levels of DNA 8-oxo-7,8- dihydro-2′-deoxyguanosine (8-oxodG) (3). In *HTT* knock-in R6/2 or R6/1 mouse models, replicating most of the clinical and pathophysiological hallmarks of HD (4,5), progression of the disease is associated with increased levels of DNA 8-oxodG (6). Accumulation of 8-oxodG in mitochondrial DNA of the striatum, the target tissue for neurodegeneration, is also observed in a chemical model for HD (7,8).

How oxidative stress mediates trinucleotide repeats (TNR) expansion is however not fully understood. DNA repair proteins can influence somatic CAG repeat expansion and mismatch repair (MMR) and base excision repair (BER) proteins are expansion-inducing factors in brain tissues of HD mouse models (9–13). The current model for BER-mediated TNR expansion (12) relies on initial removal of DNA 8-oxodG by the OGG1 DNA glycosylase, the incision of the resulting abasic site by the apurinic/apyrimidinic (AP)-endonuclease-1 (APE1) producing 3′OH and 5′-deoxyribosephosphate (5′-dRP) groups at the ends, gap-filling reactions and repair completion by polymerase β (POL β), flap endonuclease 1 (FEN1) and DNA ligase (LIG1) enzymes through long-patch BER pathway (LP BER). The repetitive nature of TNR regions may pose problems for LP BER. TNR sequences are prone to self-anneal and long 5′ flaps can form secondary structures (hairpins) that by inhibiting FEN1 activity (14,15) might favor integration into the genome. TNR expansion is affected by the loss of coordination between POL β and

---

*To whom correspondence should be addressed. Tel: +39 649902355; Fax: +39 649903650; Email: Margherita.bignami@gmail.com
Correspondence may also be addressed to Filomena Mazzei. Tel: +39 649902355; Fax: +39 649903650; Email: filomena.mazzei@iss.it

FEN1 (12,16) and the stoichiometry of BER enzymes is correlated with the tissue selectivity of somatic CAG expansion in R6/2 and R6/1 mice (17,18).

Each LP BER event involves the insertion of a limited number of nucleotides and the occurrence of 'toxic oxidation cycles' involving several rounds of OGG1-initiated BER has been suggested to underlie TNR expansion (19).

In oxidative stress conditions, an oxidized dNTPs pool might also affect the amount of 8-oxodG introduced into DNA during repair synthesis. Here, we report that 8-oxodGMP can be incorporated by POL β opposite adenine with formation of 8-oxodG:A mismatches. The possible contribution to TNR expansion from the MUTYH DNA glycosylase, which removes adenine incorporated opposite unrepaired 8-oxodG (20), has also been investigated. Our *in vitro and in vivo* results are consistent with a model where an oxidized nucleotide pool and MUTYH, in addition to OGG1, POL β and FEN1, all contribute to TNR expansion in non-dividing cells.

MATERIALS AND METHODS

Reagents

8-oxodGTP was obtained from TriLink (TriLink BioTechnologies, San Diego, CA 92121, USA), dNTPs were from Sigma (Sigma-Aldrich, Corporate Offices St. Louis, MO 63103, USA) and 2-OH-dATP was purchased from Jena (Jena Bioscience GmbH 07749 Jena, DE). Oligonucleotides, 5′ end labeled with 6-carboxyfluorescein (6-FAM) or Texas Red dyes, containing one or more 8-oxodG bases as internal modifications were from ThermoFisher (ThermoFisher Scientific, Ulm, Germany). Primers and unmodified oligomers were from Integrated DNA Technologies (IDT, Coralville, IA, USA). Human recombinant BER proteins OGG1 and APE1 were obtained from Trevigen (Trevigen Inc. Gaithersburg, MD 20877, USA) and LIG1 was from MyBioSource (San Diego, CA, USA).

Mice

A colony of R6/2 (21) transgenic and littermate wild-type (WT) mice was maintained at Charles River Laboratories (Calco, Italy). Male and female genotyped mice, usually not younger than 4.5 weeks of age, were delivered and housed in our animal facilities until the end of the experiments. All studies were conducted in accordance with the principles and procedures outlined in the EU (European Community Guidelines for Animal Care, DL 116/92, application of the European Communities Council Directive, 86/609/EEC), FELASA and ARRIVE guidelines. The animals were kept under standardized temperature, humidity and lighting conditions, and had free access to water and food. All efforts were made to reduce the number of animals used and to minimize their suffering.

On the 8th and 12th weeks of age, in early and frankly symptomatic phases, respectively, animals were sacrificed by cervical dislocation; the brain was removed quickly from the skull and selected brain areas (striatum, motor cortex and cerebellum) rapidly dissected out and frozen on dry ice.

Extract preparations from cells and tissues

Cell extracts from human gastric adenocarcinoma (AGS) lines were prepared (22). Striatum, motor cortex and cerebellum were dissected from 8- and 12-week- old R6/2 transgenic and WT mice. Briefly proteins were extracted by mechanical homogenization in a lysis buffer (50 mM Tris-HCl pH 7.4, 150 mM NaCl, 1 mM EDTA pH 8, 0.25% sodium deoxycholate, 1 mM NaF, 1 mM DTT, 0.5 mM PMSF, 1% NP-40) containing a cocktail of protease inhibitors (Complete mini, Roche). Protein concentrations were determined using a Bradford protein assay (Bio-Rad Laboratories, Hercules, CA, USA).

Primer extension experiments and incorporation kinetics analysis

Primer/templates were obtained by annealing 5′-end 6-FAM labeled primers to the template strand at 1:2 molar ratio (legend to the Figures and Supplementary Table S1). In a standard reaction, primer/templates (160 nM) were pre-incubated with POL β (0.1 U)(Trevigen) at 37°C for 1 min in the assay buffer (50 mM Tris-HCl, 10 mM MgCl$_2$, 10 mM KCl, 1 mM DTT, 1% glycerol), then 8-oxodGTP or dGTP and dTTP were added at increasing concentration and the reaction allowed for 1 h at 37°C. Reaction products were separated by 20% denaturing polyacrylamide gel electrophoresis (PAGE). Bands were visualized by fluorescence emission by Typhoon 9200 Gel Imager (GE healthcare, Uppsala, Sweden). Band analysis was performed by *ImageJ* software (available at http://imagej.nih.gov/ij/). The percentage of incorporated dNMP was plotted as a function of the added dNTPs. Data were fitted by Kaleidagraph software (Kaleidagraph, Synergy Corp., USA). Kinetics parameters were evaluated according to ref. (23). POL β incorporation of 2-OH-dATP was followed on a CTG repeat 100-mer (T2, Supplementary Table S1) annealed to a 22 nt primer oligomer ended at the C of the first repeat (S3).

BER of oxidative lesion in TNR by AGS cell extracts and purified enzymes

Duplex substrates were obtained by annealing S5/S7 and S8 oligomers to T2 complementary strand at 1:2 molar ratios (Supplementary Table S1). A nicked substrate was prepared by annealing a 22 nt (S1) and a 77 nt oligomer (S4) to a 100-mer complementary strand (T1) at 1:1:3 molar ratios. A 100 bp random sequence duplex containing an 8-oxodG was obtained by S6 and T3 oligomers.

For *in vitro* BER reconstitution with purified enzymes, 100 bp DNA duplexes (40 nM) containing the oxidative lesion were pre-incubated with purified OGG1 (0.25 U) and APE1 (1.5 U) at 37°C for 1 h and then incubated at 37°C for 1 h with POL β (80 nM), or POL β + LIG I (100 U) in the presence of 50 μM dNTPs in 50 mM Tris-HCl, pH 7.5, 50 mM KCl, 5 mM MgCl$_2$ buffer (buffer A). Repair reactions with AGS cell extracts were performed by incubating the OGG1/APE1-digested products in buffer A containing 50 μM dNTPs and 30 μg of cell extracts either in the absence or in the presence of purified POL β (80 nM). LIG1 (100 U) reaction was allowed after addition of ATP 4 mM. POL β was purified as described in ref. (24). Reaction products

were separated by 15% denaturing PAGE at 500 V for 2.5 h at 50°C.

MUTYH DNA-glycosylase assay and POL β-directed resynthesis

A DNA substrate containing an 8-oxodG:C and an 8-oxodG:A mispair was obtained by annealing two 36-mer oligonucleotides labeled at their 5′ ends with Texas Red (S9 in Supplementary Table S1) or with 6-FAM (S10), respectively. In a standard OGG1 assay, DNA substrate (10 nM) was incubated with the purified OGG1 (0–20 nM) in 20 mM Tris-HCl pH 8.0, EDTA 1 mM, DTT 1 mM, BSA 1 mg/ml (buffer B) at 37°C for 30 min. Human recombinant MU-TYH was obtained by expression and purification as fusion maltose binding protein as previously described (25). In a standard MUTYH activity assay the DNA substrate (10 nM) was incubated with purified MUTYH (20 nM, active fraction) in buffer B containing NaCl 80 mM at 37°C for 30 min. Reactions were stopped by NaOH addition and heating at 90°C for 5 min. For POL β directed gap-filling reactions, DNA duplexes (10 nM), previously treated with OGG1 or MUTYH and APE1 were incubated with increasing amount of POL β (0.25, 0.75 and 1U) in the presence of dNTP for 30 min at 37°C. Reaction products were resolved on 20% denaturing PAGE and gel images analyzed as described before.

A 100-mer DNA substrate containing an 8-oxodG:A mispair (S11-T4 in Supplementary Table S1) was pre-incubated with purified MUTYH (150 nM) and APE1 (1.5 U) and then further incubated (at 37°C for 1 h) with POL β (80 nM), or POL β plus LIG 1 (100 U) as indicated above.

Western blotting

Proteins extracts (40 μg) from striatum, motor cortex and cerebellum were separated on 4–12%-SDS polyacrylamide gels (Novex Pre-Cast gels, Invitrogene) and transferred to nitrocellulose membranes with a TransBlot cell apparatus (Bio-Rad). α-POL β (ab26343; 1:500, Abcam, Cambridge, UK), α-FEN1 (Abcam, Ab17993; 1:500), α-OGG1, (Abcam, Ab135940; 1:500), α-p53R2, (Abcam, Ab8105; 1:1000), APE1/Ref1 (sc5572; 1:100, Santa Cruz Biotechnology, USA), α-MUTYH (Abcam, Ab55551; 1:500) primary antibodies were used with α-β-Tubulin (Sigma, T5293; 1:2000) and α-LAMIN B1 (Abcam, ab16048; 1:10 000). Immunoreactions were detected with appropriate α-rabbit or α- mouse peroxidase-conjugated secondary antibodies (Jackson ImmunoResearch Laboratories, 1:10 000) and the ECL Western blotting detection Kit (Advansta). Signals were captured with ChemiDoc XRS system (Biorad) and quantified with Image Lab software.

Analysis of 8-oxodG by HPLC/EC

8-OxodG analysis was obtained by high-performance liquid chromatography with electrochemical detection (HPLC/EC) as previously described (7).

RESULTS

Oxidized purine triphosphates incorporation by POL β in TNR sequences

In conditions of oxidative stress the nucleotide pool is susceptible to damage and both 8-oxodGTP and 2-OH-dATP are substrates for incorporation into DNA and contribute to enhanced mutagenesis (26–28). Here, we investigated whether these oxidized triphosphates can be utilized by purified human POL β during BER at TNR sequences. In non-repetitive sequences POL β preferentially incorporates 8-oxodG opposite a template A (29–33). The capacity of POL β to use an oxidized triphosphate was analyzed by primer extension reactions and two substrates were used to evaluate incorporation of 8-oxodGMP opposite a C or A template nucleotide (Figure 1A and C). Incorporation of 8-oxodGMP was compared to that of a natural dGMP or dTMP and steady-state incorporation kinetics analysis are shown in Figure 1B and D. The efficiency of incorporation of 8-oxodGMP opposite C was 17.5-fold lower than that of dGMP. In contrast, 8-oxodGMP incorporation in front of A is disfavored only 3-fold over the canonical dTMP incorporation (Table 1).

In random sequences incorporation of 2-OH-dAMP by bacterial DNA polymerases lead to the formation of 2-OH-dA:C and 2-OH-dA:G mispairs (34,35). In contrast at repeated sequences, POL β was able to incorporate this oxidized monophosphate only opposite template T, with no apparent formation of other types of mismatches, even at high 2-OH-dATP concentrations (Figure 1E and data not shown).

We conclude that also in a TNR context 8-oxodGMP can be incorporated by POL β opposite either C or A. Similarly to a previous report in non-repeated sequences (33), an almost equivalent insertion of 8-oxodGMP and dTMP opposite A is observed. Finally the presence of 2-OH-dATP in an oxidized pool is unlikely to introduce new mispairs during POL β-mediated repair synthesis.

We then investigated whether POL β was able to form multiple 8-oxodG:C or 8-oxodG:A mispairs when 8-oxodGTP substituted dGTP in the dNTPs pool (Figure 2A and B). In a CAG/CTG primer template incorporation of 8-oxodGMP opposite C (C1) can occur (Figure 2A, lane 2). Addition of dCTP allows extension of the 8-oxodG:C mispair (lane 3). In the presence of both dCTP and dATP further incorporation of 8-oxodGMP occurred at the 2nd and 3rd C of the next repeats, indicating that multiple oxidized bases are inserted (lanes 4 and 5). As expected using unmodified dNTPs, dGTP was efficiently incorporated (lane 6) and the dG:dC terminal pair was extended by adding dCTP (lane 7) and the other dNTPs (lanes 8 and 9).

In a CTG/CAG primer template, the first 8-oxodG:C mispair (C1) (Figure 2B, lane 2) is elongated in the presence of dCTP with a clear band due to a second 8-oxodGMP incorporated opposite A (A1) (lane 3). Addition of dTTP allowed further 8-oxodGMP incorporation events opposite C with a pause in correspondence of the A2 template (lane 4 and 5). As previously observed on CAG/CTG, incorporation of dGMP and chain extension was efficient (lanes 6–9). Similar experiments were performed on a substrate containing
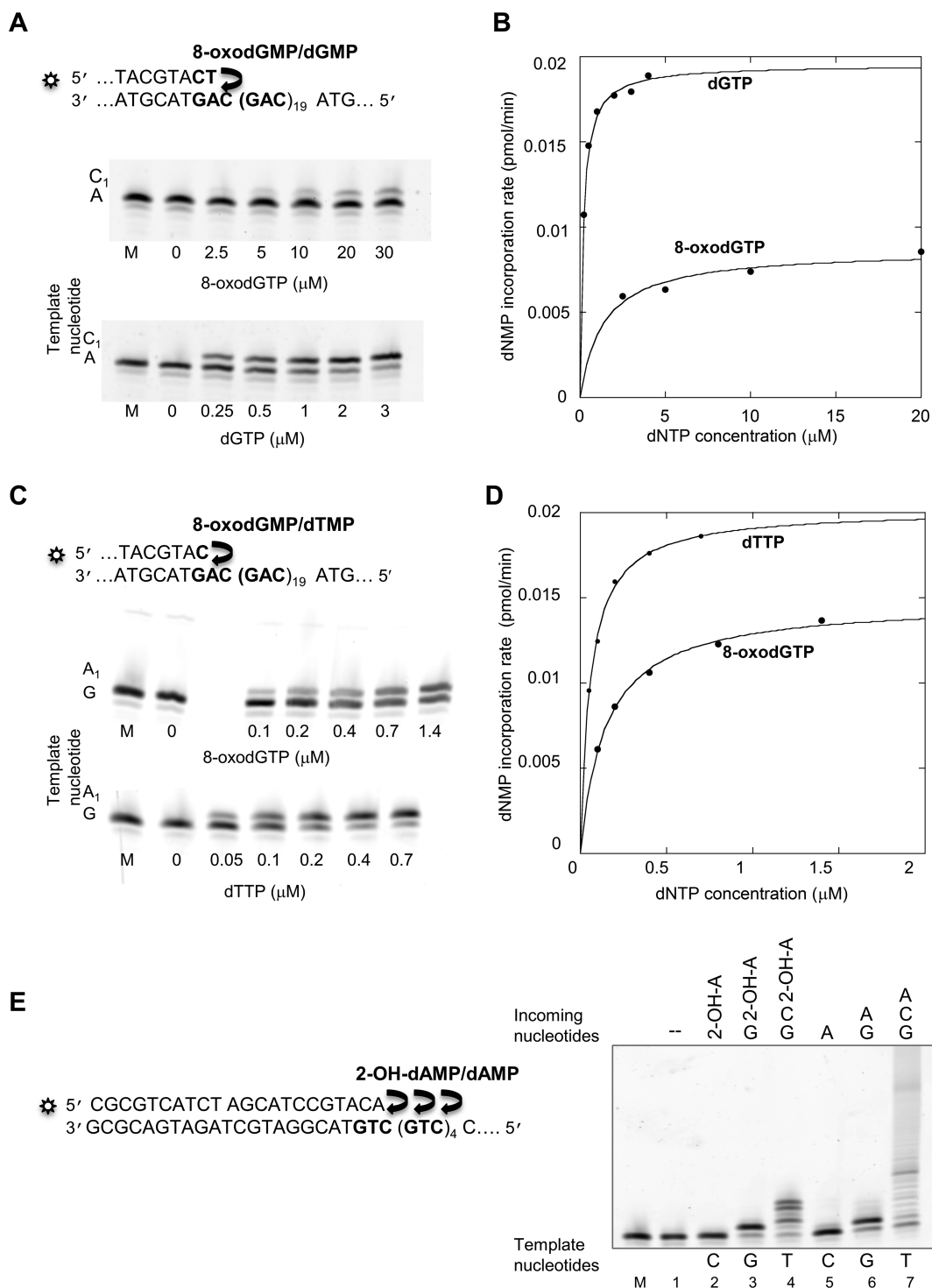
Figure 1. Incorporation of 8-oxodGMP and 2-OH-dAMP in TNR sequences. (**A** and **B**) Incorporation of dGMP and 8-oxodGMP opposite cytosine. (**A**) The primer/template sequence and representative gels are shown. Primer/template substrate (160 nM) (S1/T1) was incubated with POL β and increasing concentration of 8-oxodGTP or dGTP at 37°C for 1 h (0–30 μM and 0–3 μM, respectively). M is the DNA substrate without enzyme. Reaction products were separated by 20% denaturing PAGE at 500 V for 2.5 h. Bands were visualized by fluorescence emission by Typhoon scanner and the analysis of the band intensities was performed by *ImageJ* software. (**B**) Percentage of incorporated dNMP plotted as a function of added dNTPs. Data were fitted by Kaleidagraph software to evaluate kinetics parameters. (**C** and **D**) Incorporation of 8-oxodGMP and dTMP opposite adenine. Primer/template sequences is S2/T1 (Supplementary Table S1). Experimental conditions and analyses were as described above. The concentration range of 8-oxodGTP and dTTP was 0–2 μM and 0–1 μM, respectively. (**E–F**) Incorporation of 2-OH-dAMP and dAMP in CAG/CTG repeat sequence. (**E**) Primer/template sequence is S3/T2 (Supplementary Table S1); (**F**) Primer/template duplex (160 nM) was incubated with POL β (0.1U) in 10 μl reaction buffer in the absence of dNTP (lane 1), after addition of 2-OH-dATP (lane 2), dGTP and 2-OH-dATP (lane 3); 2-OH-dATP, dGTP and dCTP (lane 4), dATP (lane 5); dATP and dGTP (lane 6), dATP, dGTP and dCTP (lane 7). All nucleotide triphosphates were at 10 μM final concentration. Reaction products were separated by 15% denaturing PAGE and image acquisition and analysis was performed as described before.

Table 1. Kinetic parameters for incorporation of 8-oxodGMP in a CAG repeat template by POL β

Sample	dNTP	K_m (μM)	V_{max} (pmol min^{-1})	f_{inc}	Selectivity index
1	8-oxodGTP	1.38 ± 0.36	0.0087 ± 0.0004	5.7×10^{-2}	17.5
	dGTP	0.18 ± 0.02	0.0195 ± 0.0004		
2	8-oxodGTP	0.15 ± 0.01	0.0015 ± 0.0003	29.3×10^{-2}	3.4
	dTTP	0.057 ± 0.004	0.0020 ± 0.0003		

[1]Primer/template obtained by annealing S1 and T1 strand (reported in Supplementary Table S1).
[2]Primer/template obtained by annealing S2 and T1 strands (reported in Supplementary Table S1).
f_{inc} is the incorporation frequency, calculated as $(V_{max}/K_m)_{\text{8-oxoGTP}}/(V_{max}/K_m)_{dGTP}$; selectivity index is defined as $1/f_{inc}$.
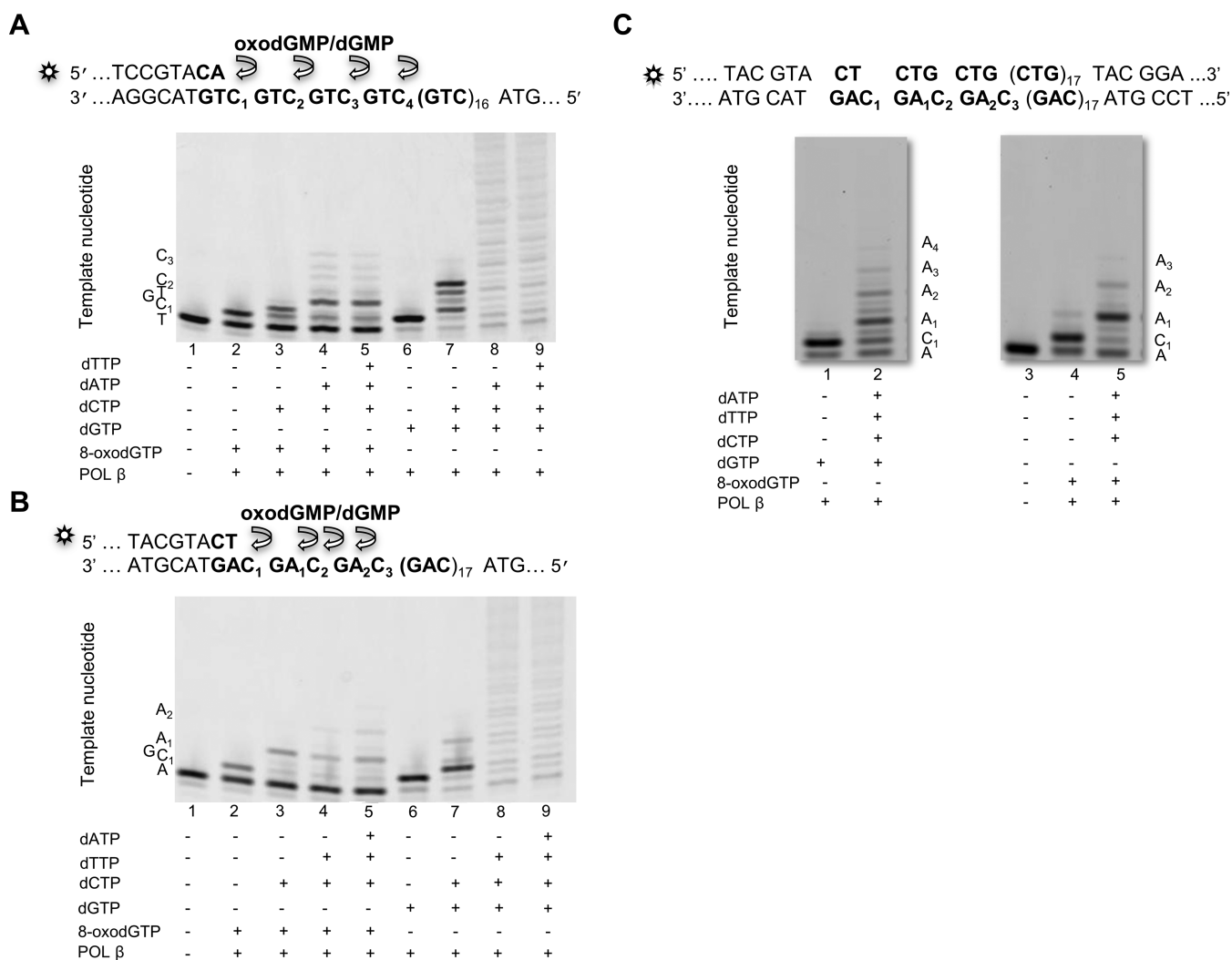
Figure 2. Incorporation and extension of 8-oxodGMP by POL β. Primer/template (160 nM) (Supplementary Table S1, S3/T2 panel A; S1/T1 panel B) were used. Both substrates were incubated with POL β (0.1 U) and 8-oxodGTP or dGTP and others dNTPs (50 μM final concentration each). (**A**) Lane 1, primer; lane 2, 8-oxodGTP; lane 3, as lane 2 plus dCTP; lane 4, as lane 3 plus dATP; lane 5, as lane 4 plus dTTP; lane 6, primer plus dGTP; lane 7, as lane 6 plus dCTP; lane 8 as lane 7 plus dATP; lane 9, as lane 8 plus dTTP. (**B**) Lane 1, primer; lane 2, primer plus 8- oxodGTP; lane 3, as lane 2 plus dCTP; lane 4 as lane 3 plus dTTP; lane 5, as lane 4 plus dATP; lane 6, primer plus dGTP; lane 7, as lane 6 plus dCTP; lane 8 as lane 6 plus dTTP and dATP. (**C**) The DNA substrate (160 nM) was built by annealing three oligomers of 22, 77 and 100 bases respectively indicated as S1, S4 and T1 in Supplementary Table S1, in order to produce a preformed nicked duplex containing CTG/CAG repeats. Incorporation of dGTP and 8-oxodGTP (lanes 1 and 4) and elongation (lanes 2 and 5) was obtained by incubating the substrate (lane 3) with POL β (0.1 U) at 37°C for 1 h.

a gap in the CTG/GAC repeats (Figure 2C). It has been shown that repair synthesis by POL β occurs via LP BER pathway at repeated sequences (16). We confirmed these results and, after the initial insertion of a G opposite C1, the repair patch contained more than 10 nucleotides (Figure 2C, lanes 1 and 2). When dGTP was substituted with 8-oxodGTP, multiple mismatches containing the oxidized purine were formed by POL β (lanes 3–5).

In conclusion these results indicate that, in the presence of oxidized dNTPs, repair synthesis by POL β results in the formation of clustered oxidative lesions introduced into repeated sequences.

Effects of an oxidized pool on expansion of TNR sequences during BER

We then investigated whether 8-oxodGTP can be inserted during POL β-mediated repair synthesis and allow expansion of a TNR-containing substrate. We initially verified on a consolidated model system whether TNR expansion occurred in the presence of purified BER proteins and unmodified dNTPs (16). A 100 bp DNA duplex containing 20 CAG repeats and a single 8-oxodG located in the first repeat unit was reacted with purified OGG1 and APE1 (Figure 3, panel A, lane 1) and the nicked duplex was incubated either with POL β (lane 2) or with POL β supplemented with LIG1 (lane 3 and 4). Reaction products were then analyzed by denaturing PAGE and single stranded oligonucleotides of 100 nt, 109 nt, 115 nt were used as markers. Processing of the cleaved substrate by POL β resulted in the formation of repair intermediates (RI) containing more than 5 TNR (shown by densitometric scans at the bottom of the gel). Following LIG1 addition, RI were resolved into products longer than 100-mer (duplicate runs in lane 3 and 4). A close-up view of the densitometric scans of the region containing 100–115 nt (panels on the right of the gel) also points out the shift in molecular weights of repair products consistent with an expanded substrate. In contrast, and as previously reported (16), no products longer than 100 nt were observed when 8-oxodG was located in a random sequence (Supplementary Figure S1, lane 3 and 4). In this case the lesion was essentially repaired *via* short-patch BER.

It has been shown that expansion of repeated sequences, initiated by an OGG1-mediated repair event, can be modulated by BER protein stoichiometry (16–18). Thus, BER was studied in AGS cell extracts in the presence or the absence of additional purified POL β. These gastric cancer cells contain increased levels of APE1 and POL β BER proteins (8-fold and 2-fold, respectively, in comparison to mouse embryo fibroblasts) (Supplementary Figure S2). When the OGG1/APE1-treated model substrate (Figure 3B, lane 1) was incubated with AGS cell-free extracts supplemented with canonical dNTPs, a limited number of RI containing up to two TNR was observed (lane 2). When the stoichiometry of BER factors was further altered by supplementing the extracts with purified POL β, RI containing more than 5 TNR were observed (lane 4). After LIG1 supplementation, full-length products longer than 100 nt were obtained (lanes 3 and 5). Densitometric scans of the various lanes showing modulation of RI are presented at the bottom of the gel. Panels on the right of the gel show

the shift in molecular weights of repair products consistent with an expanded substrate.

When POL β-supplemented AGS extracts were incubated with dNTPs where 8-oxodGTP substituted dGTP, the number of RI was only slightly reduced in comparison to the pattern observed with canonical dNTPs (Figure 3C, lanes 2 and 4, respectively and densitometric scans at the bottom of the gel). In agreement with previous results (16) POL β-mediated DNA synthesis caused a pattern of periodicity with pausing occurring after dAMP incorporation (Figure 3C, lane 2). In addition to the regular pausing at adenine, further pausing after 8-oxodGMP addition was detectable (Figure 3, compare lane 2 and 4). After LIG1 supplementation, the reaction products display a broad length distribution with fragments longer than 100 nt in both cases (lanes 3 and 5 and densitometric scans on the right of the gel).

In conclusion, repair synthesis by POL β supplemented-AGS cell extracts in the presence of 8-oxodGTP results in the formation of multiple mispairs containing oxidized bases, with a minor limitation of TNR expansion.

To investigate whether multiple insertion of 8-oxodGMP in the same DNA duplex could be further processed by BER, 100-mers with two 8-oxodG located at a distance of 2 or 7 TNR were annealed to the complementary strand and the resulting duplexes were used as substrates for repair synthesis reactions following digestion with OGG1 and APE1 (Figure 4A and B). The majority of the products, most likely derived from doubly nicked substrates, run as a 22 nt and only a small amount of singly cleaved molecules at the 8-oxodG in position 31 or 46 was observed (Figure 4A and B, lanes 2). Incubation of these substrates with AGS cell extracts produced several RI starting from both cleaved sites (lanes 3). Further addition of POL β resulted in RI of increased length in both substrates (lanes 4). Thus, multiple and closely spaced oxidized lesions inserted during POL β-mediated repair synthesis can be independently processed in further rounds of OGG1-initiated BER.

POL β-dependent repair synthesis from MUTYH-initiated BER

Since POL β incorporation of 8-oxodGMP lead to the formation of 8-oxodG:A mispairs we verified whether a purified human MUTYH was able to remove the A opposite 8-oxodG in the TNR sequence. A 36 bp duplex with an 8-oxodG:C mispair at the first of six CTG/GAC repeats and an 8-oxodG:A mispair at the fifth CTG/GAC repeat was constructed with Texas red and 6-FAM dye at the 5′ of the 8-oxodG and A strand, respectively (Figure 4C). The OGG1 and MUTYH potential cleavage sites are indicated in panel C with a red and a green arrow, respectively. Incubation of the duplex substrate with increasing concentrations of OGG1 (Figure 4D lanes 1–4) led to the formation of the expected 12 nt cleavage product and the integrity of the bottom strand (green band in the gel image) confirmed the substrate specificity of this enzyme. When MUTYH activity was investigated, an increase of the specific cleavage product paralleled the disappearance of the full-length substrate (top green band in Figure 4E). The cleavage is specific and no fragments deriving from digestion on the comple-

☀5′ ...CCGTA **CAG*** **(CAG)**₁₉ TACGT...3′
3′ ...GGCAT **GTC** **(GTC)**₁₉ ATGCA...5′
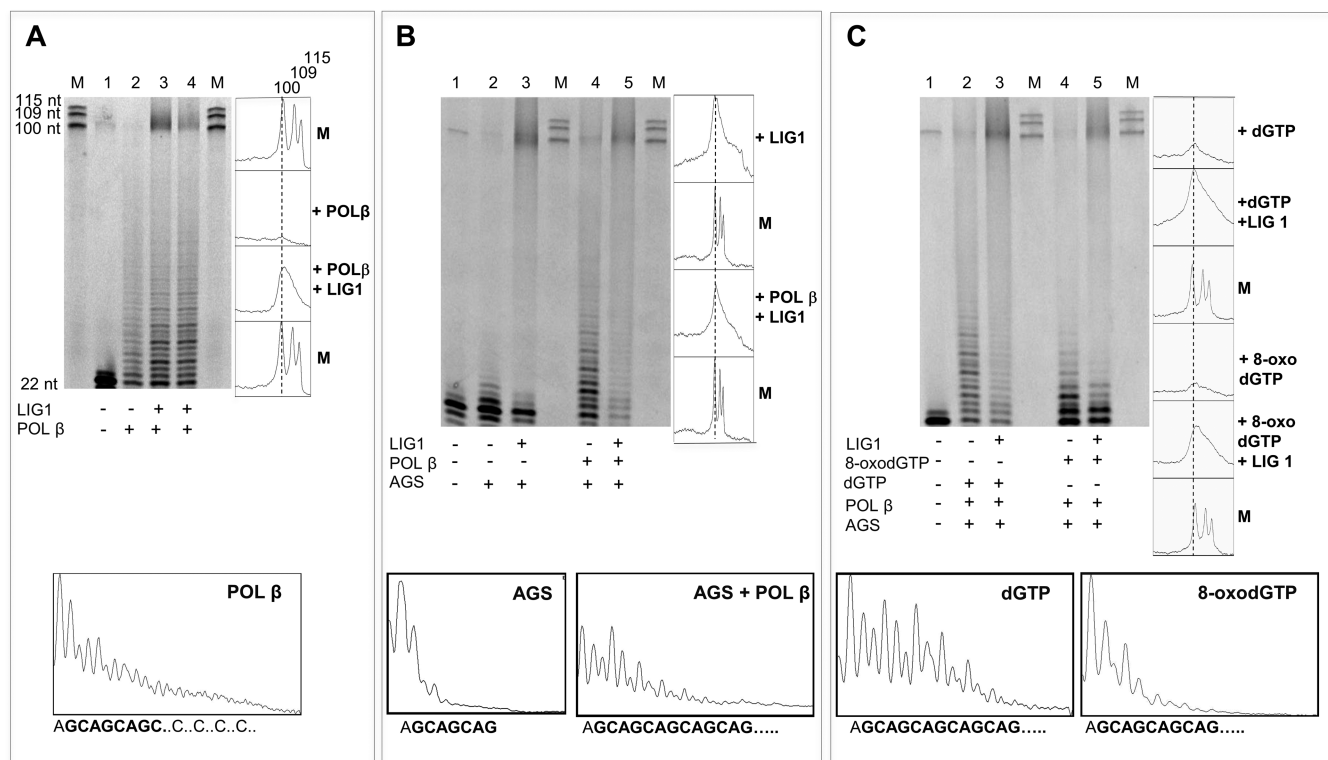
Figure 3. TNR expansion by purified proteins and AGS cell extracts. A 100 bp duplex, 5′-end 6-FAM labeled, containing 20 CAG repeats and a single 8-oxodG (G*) (S5 and T2 oligomers in Supplementary Table S1) was pre-incubated with OGG1 and APE1 enzymes (Panels **A**–**C**, lanes 1) and then further processed in the conditions described below. Reaction products were separated by 15% denaturing PAGE. M is a mix of 100 nt, 109 nt and 115 nt markers. (**A**) POL β (lane 2) and duplicate runs of samples containing POL β plus LIG1 (lanes 3–4). Densitometric profiles of RI in lane 2 are shown at the bottom of panel A. A close-up view of the densitometric scan of lanes 2 and 3 in the 100–115 nt region is shown at the right of the gel. (**B**) AGS cell extracts (30 μg) (lane 2); AGS extracts supplemented with LIG1 alone (lane 3), or supplemented with POL β (lane 4), and POL β plus LIG1 (lane 5). Densitometric profiles of RI in lanes 2 and 4 are at the bottom of panel B. Densitometric scan of lanes 3 and 5 in the 100- 115 nt region is shown at the right of the gel. (**C**) AGS cell extracts supplemented with POL β in the presence of dGTP (50 μM) (lane 2), oxidized dGTP (500 μM) (lane 4) and the other dNTPs (50 μM); LIG1 supplementation is in lane 3 and 5. Densitometric profiles of RI in lanes 2 and 4 are reported at the bottom of the gel, those in the 100–115 nt region are on the right.

mentary strand were observed also in this case (red band in the gel image). When the products of MUTYH/APE1 reaction were incubated with increasing concentration of POL β, longer RI were observed, while a residue product at +1 nt position was still present (Figure 4F, lanes 1–3). The green arrow at the top of the gel indicates the borderline position with the random sequence (last nine nucleotides in the sequence).

We then verified whether the MUTYH-dependent incision of an 8-oxodG:A mispair triggered TNR expansion in the presence of other BER factors. A 100-mer substrate containing 20 repeats with the last one being an 8-oxodG:A mismatch was constructed (Figure 4G). Following incision with MUTYH and APE1 (Figure 4H, lane 1), expansion products were identified after POL β and ligase supplementation (lanes 2–4). Thus MUTYH can efficiently recognize and specifically incise 8-oxodG:A mispairs in a TNR sequence. In addition, the incorporation of several nucleotides by POL β resembles the LP BER of OGG1-mediated repair of 8-oxodG:C mismatch in TNR sequences.

DNA 8-oxodG and repair proteins levels in WT an R6/2 mouse brains

We then studied whether the conditions necessary for TNR expansion by aberrant BER processing were present in a mouse model for HD. We used the R6/2 transgenic mouse, which expresses exon 1 of the human HD gene with around 150 CAG repeats, and exhibits a progressive neurological phenotype (21). The expression level of several DNA repair proteins was then compared in WT and R6/2 mice. Areas affected (striatum and motor cortex) and non-affected (cerebellum) by TNR expansion were analyzed and representative westerns together with the results from four mice/genotype are shown in Figure 5. Both MUTYH and OGG1 DNA glycosylases were expressed in all these areas with no significant difference between wild-type and R6/2 mice (Figure 5A–C). Similarly the genotype did not influence the level of expression of these enzymes in the motor cortex of 12-week old animals (Figure 5D). This indicates that the first steps in the recognition and processing of 8-
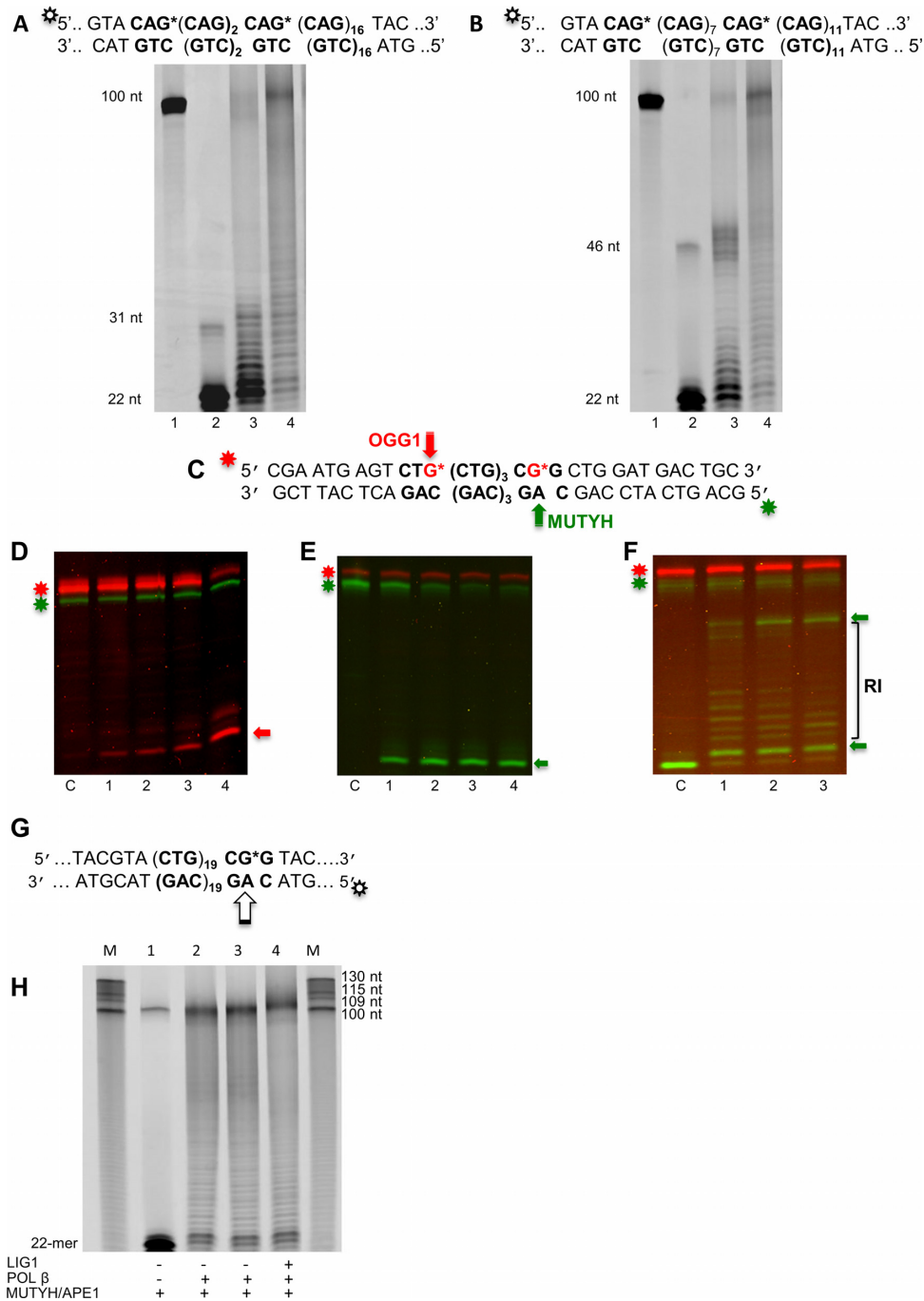
Figure 4. LP BER in TNR repeats containing multiple oxidative lesions and 8-oxodG:A repair. The 100 bp duplexes, labeled at the 5′ end with 6-FAM (160 nM), containing 20 uninterrupted CAG repeats and two 8-oxodG bases (indicated as G*) were used. To obtain a different separation between the lesions, 8-oxodG were located at the (**A**) 1st and 4th repeat or at the (**B**) 1st and 9th repeat. The complete sequences of the oligomers are S7 and S8 (G* strand) and T2 (complementary strand)(Supplementary Table S1). (**A** and **B**) untreated samples (lanes 1); samples incubated with OGG1 and APE1 (lanes 2); products obtained after substrate incubation with AGS extracts (lanes 3) and AGS extract supplemented with POL β (lanes 4). Reaction products were separated by 15% denaturing PAGE. (**C**) A 36-mer DNA substrate containing an 8-oxodG:C and an 8-oxodG:A mispair in a CTG/CAG repeat context (S9 and S10 oligomers in Supplementary Table S1). Top strand containing the oxidative lesions was 5′ end labelled with Texas red dye; bottom strand was 5′ end labeled with 6-FAM. The red and green arrows indicate the putative excision sites of OGG1 and MUTYH enzymes respectively. (**D**) DNA substrate (10 nM) was reacted with increasing concentrations of purified OGG1 (0–20 nM) at 37°C for 30 min. (**E**) DNA substrate (10 nM) reacted with increasing concentration of purified MUTYH (0–20 nM) at 37°C for 30 min. (**F**) POL β-directed gap-filling. DNA duplex (10 nM) previously treated with MUTYH and APE1 was incubated with increasing amounts of POL β (0.25, 0.75 and 1 U respectively in lanes 1–3) and 50 μM dATP, dCTP and dGTP for 30 min at 37°C. Reaction products were separated by 20% denaturing PAGE. The star and the arrow indicate the full-length oligomer and the reaction products positions, respectively. (**G**) The 100 bp substrate containing a single 8-oxoG:A mispair obtained by annealing S11 and T4 oligomers (Supplementary Table S1); the green arrow indicates the the potential excision site of MUTYH. (**H**) The DNA substrate pre-incubated with MUTYH and APE1 (lane 1) was incubated with POL β (duplicate runs in lanes 2 and 3) and POL β plus LIG1 (lane 4) in the presence of 50 μM dNTPs. M was a mixture of markers of different size.
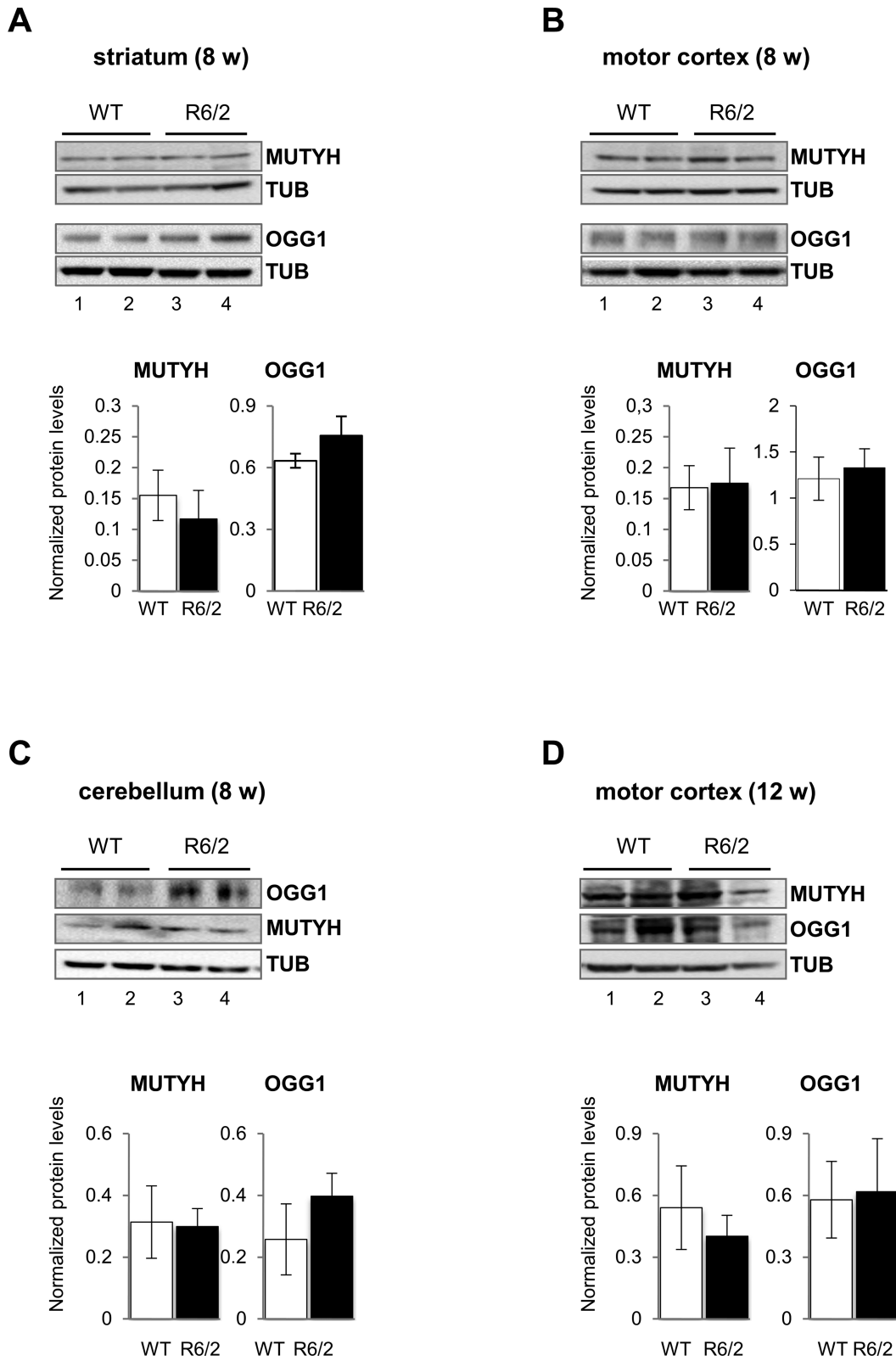
Figure 5. Western blot analysis of OGG1 and MUTYH protein levels in brain areas of WT and R6/2 mice. Western blot analyses of OGG1 and MUTYH proteins in whole extracts prepared from (**A**) striatum, (**B**) motor cortex, (**C**) cerebellum of 8 week-old WT and R6/2 mice. (**D**) Expression of the same genes in extracts prepared from the motor cortex of 12 week-old WT and R6/2 mice. Data in lanes 1–2 and 3–4 are derived from 2 WT and 2 R6/2 mice, respectively. The graphs show the quantification of Western blottings as ratios of DNA repair protein levels to tubulin (TUB). These data were obtained from independent extracts from 4 WT and 4 R6/2 mice. WT mice (WT, open bar); R6/2 mice (black bar).

oxodG-containing mismatches are unaffected by HTT expression.

When POL β and FEN1 protein levels were analyzed in the same brain areas, POL β levels were significantly lower in the striatum and motor cortex of R6/2 mice than in WT mice at 8 weeks of age (Supplementary Figure S3A and B) and this difference was maintained in the motor cortex of disease mice at later times (12 weeks) (Supplementary Figure S3D, lanes 1–3 versus 2–4 and relative histograms). In the cerebellum unaffected by TNR expansion, POL β levels were similar in WT and R6/2 mice (Supplementary Figure S3C, lanes 1–2 versus 3–4). FEN1 levels were only slightly increased by mutant *HTT* expression in striatum and motor cortex (Supplementary Figure S3A, B and D). It is noticeable however that in WT mice the ratio between POL β and FEN1 is >1, while an inverse trend is observed in these brain areas of R6/2 mice. This does not occur in the cerebellum (Supplementary Figure S3C). As already observed in R6/1 mice (17), tissue specific differences in POL β and FEN1 protein levels are present in brain areas of R6/2 mice. Thus, modification in the levels of POL β and FEN1 repair proteins in affected areas is coherent with an unbalanced BER associated with disease occurrence in R6/2 mice (17,18).

To verify whether increased DNA oxidation is present in mice undergoing TNR expansion, the levels of brain DNA 8-oxodG were compared in 12-week old WT and R6/2 mice (Figure 6A and B). Compared to WT mice, DNA 8-oxodG levels were 1.4- and 1.9-fold higher in the R6/2 mouse striatum and motor cortex, respectively. When similar analyses were performed in the striatum of younger R6/2 mice (8-week old) similar levels of the oxidized purine were identified (0.36 ± 0.04 versus $0.32 \pm 0.03 \times 10^6$ dG at 8 and 12 weeks, respectively). This indicates that an increased level of DNA damage is an early event in this HD mouse model.

Finally to investigate whether the dNTPs pool in the brain of R6/2 mice was exposed to an oxidative stress, we measured the level of the p53-inducible ribonucleotide reductase (p53R2). This enzyme is responsible for providing deoxyribonucleotides to quiescent cells exposed to genotoxic damage (36–38). Affected areas of 8-week old R6/2 (striatum and motor cortex) contained higher levels of p53R2 than the same areas in WT mice (Figure 6C and D). Conversely, no increase in p53R2 expression was identified in non-affected areas such as the cerebellum (Figure 6E).

Thus, together with high levels of oxidized bases in the genome, we provide a strong indication of an oxidized dNTPs pool being present in the areas affected by neurodegeneration in this mouse model for HD.

DISCUSSION

The role of DNA repair in modulating TNR expansion has been extensively investigated and several *in vivo* and *in vitro* observations indicate that repair factors can affect the length of repeat tracts in HD, myotonic dystrophy and Fragile X-related disorders models (9,4,11–13,39–41). These include some MMR factors as well as enzymes involved in BER of oxidized bases such as OGG1, NEIL1 and POL β (12,13,41,42). Here, we confirm the involvement of BER enzymes in TNR expansion (12,13,16,17). We also identified the oxidized dNTP pool as a source of multiple DNA mismatches leading to processing on both DNA strands by the MUTYH and OGG1 DNA glycosylases, suggesting that these glycosylases might play a role in TNR expansion.

We propose a novel model that integrates previous ones (12,40,43) (Figure 7). After an initial OGG1/APE1-mediated strand break, during POL β-dependent repair synthesis the downstream strand is progressively displaced and results in the formation of a flap. Due to the self-annealing property of TNR repeats as the flap length increases, because of the progression of the polymerase, the flap may fold. When the overall length of the flap is >3 TNR, flap alternates between folded and unfolded conformations. At longer repeats stable hairpins can be formed which constitute a hindrance to FEN1 activity (14,15). Here, we show that, during repair synthesis in the presence of an oxidized dNTPs pool, incorporation of 8-oxodGMP and its extension can result in clusters of 8-oxodG occurring in the same strand. In addition, due to the ascertained capacity of POL β to incorporate 8-oxodGMP opposite A, 8-oxodG:A mispairs can also be formed. Removal of A from the 8-oxodG:A mismatch by MUTYH DNA glycosylase initiates an independent round of BER with possible formation of a hairpin in the opposite strand. After ligation, this will favor the realignment into the sequence of the extra repeats, thus generating an expansion event in the absence of DNA replication. Processing of 8-oxodG:C and 8-oxodG:A mispairs located in close proximity by the OGG1 and MUTYH DNA glycosylases suggests that clustered lesions of this type can concur to TNR expansion. Recently we showed that POL β erroneously incorporates oxidized ribonucleotides in a TNR-containing sequence creating new substrates for MUTYH (44). Whether this also contributes to the expansion process remains to be ascertained. Finally, extrahelical CAG/CTG elements can also trigger the activation of the MMR MutSβ and MutLα complexes (45,46), possibly misdirecting the MMR process and resulting in TNR expansion (47). It is presently unknown whether the non-canonical BER and MMR pathways are mutually exclusive or both contribute to repeat expansion in non-replicating DNA.

An important part of our report is the demonstration that the requirements for our proposed expansion mechanism (i.e. the DNA repair factors, oxidized DNA and oxidized dNTP) are all present in brain areas affected by neurodegeneration in the R6/2 mouse model of HD. Oxidative stress produced by mutant HTT, a recognized feature of HD and the increased levels of DNA 8-oxodG identified in the genome of striatum and motor cortex of R6/2 mice are consistent with ROS selectively affecting some brain areas where TNR expansion occurs. Although in differentiated tissues the intracellular concentration of dNTPs is several-fold lower than during the S- phase (48), dNTPs levels must be sufficient for mitochondrial DNA synthesis and repair of DNA damage. Indeed in the presence of genotoxic damage deoxyribonucleotides of quiescent cells are provided mainly via the salvage pathway by a ribonucleotide reductase containing a p53-inducible R2 subunit (36–38). It is interesting that a DNA damage response is indeed fully activated in HTT cellular models (49). Although the information on
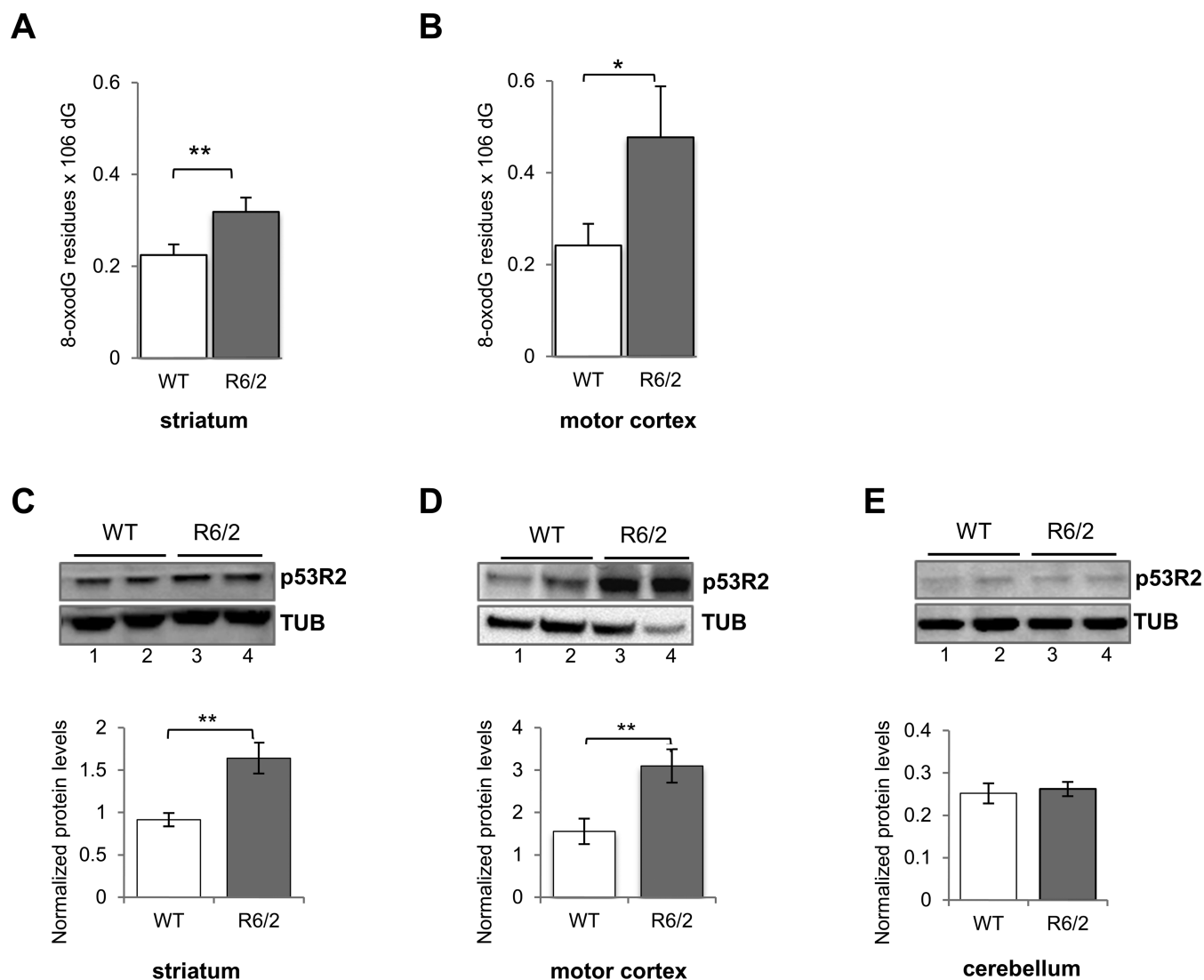
Figure 6. Steady-state levels of 8-oxodG and expression of the p53R2 protein in brain areas of wild-type and R6/2 mice. Groups of WT (n = 10) and R6/2 mice (n = 10) were sacrificed and levels of 8-oxo-dG were determined by HPLC-EC in genomic DNA prepared from the indicated brain areas. DNA 8-oxodG levels in (**A**) striatum and (**B**) motor cortex of 12 week-old WT (WT, open bar) and R6/2 mice (grey ba**r**). Data are the mean±SE. The asterisks indicate significant differences by Student's *t*-test (*$P < 0.05$; **$P < 0.02$). Western blot analyses of p53R2 in whole extracts prepared from (**C**) striatum, (**D**) motor cortex and (**E**) cerebellum of WT and R6/2 mice. Data in lanes 1–2 and 3–4 are derived from 2 WT and 2 R6/2 mice, respectively. The graphs show the quantification of Western blottings as ratios of DNA repair protein levels to TUB. Error bars indicate mean±SD from 3–4 independent determinations.

8-oxo-dGTP levels in the brain is limited to rat mitochondrial dNTP pools, the identified trace amounts of 8-oxo-dGTP have been shown to be sufficient to reduce DNA polymerase γ replication fidelity (50). We propose that in disease mice the levels of oxidized triphosphates might be much higher and contribute to the disease. Supportive evidence on the role of the oxidized dNTPs pool in neurodegenerative conditions comes from the work on mice defective or overexpressing MTH1, the hydrolase that degrades 8-oxodGTP and 8-oxoGTP and prevents accumulation of 8-oxoG in DNA and RNA (51,52). An increased sensitivity of $Mth1^{-/-}$ animals has been indeed shown in a mouse model for Parkinson's disease (53), in kainate-induced excitotoxicity (54), inherited retinal degeneration (55), while hMTH1-overexpressing mice are resistant to NP- induced

HD-like striatal neurodegeneration (7). The role of oxidized pool might help in explaining some unresolved questions about the onset of largely extended CTG/CAG repeated regions. The levels of 8-oxodG induced by oxidant exposures (in the range of $2–10 \times 10^{-6}$ Guanines) makes it unlikely that multiple, closely spaced 8-oxodG lesions are the result of direct damage to the bases. Experimental evidence in cultured cells indicates that the nucleotide pool is a significant target for oxidative stress (56). OGG1 and MUTYH repair proteins are also expressed in several brain areas. This is not surprising in the case of OGG1, which is active in the repair of 8-oxodG:C mismatches throughout the cell cycle. In contrast, in cells in culture, MUTYH is expressed only during the S phase of the cell cycle (57). In the brain, however, where replication is mainly restricted to mitochondria, MU-
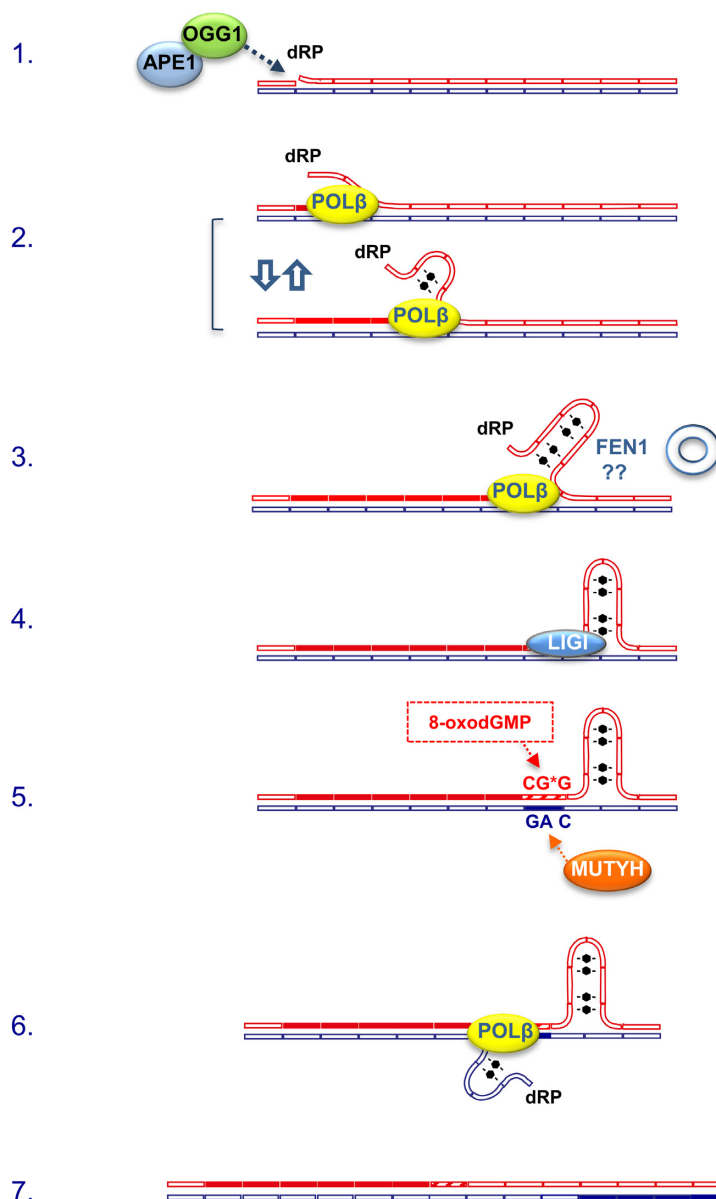
Figure 7. Novel contributors in TNR expansion process. Following an initial incision event mediated by OGG1 and APE1 at an 8-oxodG site in the top strand (red, step 1), POL drives repair synthesis by LP BER. Long flaps might eventually fold in stable secondary structures (step 2). A faulty removal by FEN1 depending on flap conformations might leave hairpins with unligatable dRP ends (step 3). Removal of dRP by POL β allows ligation by LIG1 (step 4). If 8-oxodGTP is present in the dNTPs pool, 8-oxodGMP can be incorporated opposite A in the complementary strand creating a substrate for MUTYH (step 5). MUTYH activity on the bottom strand (blue) allows the initiation of a new repair event, as well as an elongation process on this side (step 6). Realignments of the strands will result in TNR expansion (step 7). Newly synthesized tracts are represented by full rectangles. The proposed model has been modified from refs. (12,16,40).

TYH expression is probably necessary for repairing DNA damage in these organelles. In the presence of excessive oxidative damage MUTYH-mediated intervention might become toxic. Although no information is available on a direct involvement of MUTYH in TNR expansion, the 3-NP neurotoxicity observed in *Ogg1*$^{-/-}$ mice is dependent on an active MUTYH in a chemical model for HD (58). In conclusion we propose that in the presence of oxidative stress, MUTYH, analogously to OGG1, might play a toxic role in the nucleus in modulating triplet-mediated expansion.

SUPPLEMENTARY DATA

Supplementary Data are available at NAR Online.

REFERENCES

1. Lin,M.T. and Beal,M.F. (2006) Mitochondrial dysfunction and oxidative stress in neurodegenerative diseases. *Nature*, **443**, 787–795.
2. Duyao,M., Ambrose,C., Myers,R., Novelletto,A., Persichetti,F., Frontali,M., Folstein,S., Ross,C., Franz,M., Abbott,M. *et al.* (1993) Trinucleotide repeat length instability and age of onset in Huntington's disease. *Nat. Genet.*, **4**, 387–392.
3. Polidori,M.C., Mecocci,P., Browne,S.E., Senin,U. and Beal,M.F. (1999) Oxidative damage to mitochondrial DNA in Huntington's disease parietal cortex. *Neurosci. Lett.*, **272**, 53–56.
4. Wheeler,V.C., Auerbach,W., White,J.K., Srinidhi,J., Auerbach,A., Ryan,A., Dutao,M.P., Vrbanac,V., Weaver,M., Gusella,J.F. *et al.* (1999) Length-dependent gametic CAG repeat instability in the Huntington's disease knock-in mouse. *Hum. Mol. Genet.*, **8**, 31–35.
5. Brouillet,E., Conde,F., Beal,M. and Hantraye,P. (1999) Replicating Huntington's disease phenotype in experimental animals. *Prog. Neurobiol.*, **59**, 427–468.
6. Bogdanov,M.B., Andreassen,O.A., Dedeoglu,A., Ferrante,R.J. and Beal,M.F. (2001) Increased oxidative damage to DNA in a transgenic mouse model of Huntington's disease. *J. Neurochem.*, **79**, 1246–1249.
7. De Luca,G., Russo,M.T., Degan,P., Tiveron,C., Zijno,A., Meccia,E., Ventura,I., Mattei,E., Nakabeppu,Y., Crescenzi,M. *et al.* (2008) A role for oxidized DNA precursors in Huntington's disease-like striatal neurodegeneration. *PLoS Genet.*, **4**, e1000266.
8. Ventura,I., Russo,M.T., De Nuccio,C., De Luca,G., Degan,P., Bernardo,A., Visentin,S., Minghetti,L. and Bignami,M. (2012). hMTH1 expression protects mitochondria from Huntington's disease-like impairment. *Neurobiol. Dis.*, **49**, 148–158.
9. Manley,K., Shirley,T.L., Flaherty,L. and Messer,A. (1999) Msh2 deficiency prevents in vivo somatic instability of the CAG repeat in Huntington disease transgenic mice. *Nat. Genet.*, **23**, 471–473.
10. Wheeler,V.C., Lebel,L.A., Vrbanac,V., Teed,A., te Riele,H. and MacDonald,M.E. (2003) Mismatch repair gene Msh2 modifies the timing of early disease in Hdh(Q111) striatum. *Hum. Mol. Genet.*, **12**, 273–281.
11. Dragileva,E., Hendricks,A., Teed,A., Gillis,T., Lopez,E.T., Friedberg,E.C., Kucherlapati,R., Edelmann,W., Lunetta,K.L., MacDonald,M.E. *et al.* (2009) Intergenerational and striatal CAG repeat instability in Huntington's disease knock-in mice involve different DNA repair genes. *Neurobiol. Dis.*, **33**, 37–47.
12. Kovtun,I.V., Liu,Y., Bjoras,M., Klungland,A., Wilson,S.H. and McMurray,C.T. (2007) OGG1 initiates age-dependent CAG trinucleotide expansion in somatic cells. *Nature*, **447**, 447–452.
13. Budworth,H., Harris,F.R., Williams,P., do Lee,Y., Holt,A., Pahnke,J., Szczesny,B., Acevedo-Torres,K., Ayala-Peña,S. and McMurray,C.T. (2015) Suppression of somatic expansion delays the onset of pathophysiology in a mouse model of Huntington's disease. *PLoS Genet.*, **11**, e1005267.
14. Spiro,C., Pelletier,R., Rolfsmeier,M.L., Dixon,M.J., Lahue,R.S., Gupta,G., Park,M.S., Chen,X., Mariappan,S.V. and McMurray,C.T. (1999) Inhibition of FEN-1 processing by DNA secondary structure at trinucleotide repeats. *Mol. Cell*, **4**, 1079–1085.
15. Henricksen,L.A., Tom,S., Liu,Y. and Bambara,R.A. (2000) Inhibition of flap endonuclease 1 by flap secondary structure and relevance to repeat sequence expansion. *J. Biol. Chem.*, **275**, 16420–16427.
16. Liu,Y., Prasad,R., Beard,W.A., Hou,E.W., Horton,J.K., McMurray,C.T. and Wilson,S.H. (2009) Coordination between polymerase beta and FEN1 can modulate CAG repeat expansion. *J. Biol. Chem.*, **41**, 28352–28366.
17. Goula,A., Berquist,B.R., Wilson,D.M. III, Wheeler,V.C., Trottier,Y. and Merienne,K. (2009) Stoichiometry of base excision repair proteins correlates with increased somatic CAG instability in striatum over cerebellum In Huntington's disease transgenic mice. *PLoS Genet.*, **5**, e1000749.
18. Goula,A.V., Pearson,C.E., Della Maria,J., Trottier,Y., Tomkinson,A.E., Wilson,D.M. III and Merienne,K. (2012) The nucleotide sequence, DNA damage location, and protein stoichiometry influence the base excision repair outcome at CAG/CTG repeats. *Biochemistry*, **51**, 3919–3932.
19. McMurray,C.T. (2010) Mechanisms of trinucleotide repeat instability during human development. *Nat. Rev. Genet.*, **11**, 786–799.
20. Mazzei,F., Viel,A. and Bignami,M. (2013) Role of MUTYH in human cancer. *Mutat. Res.*, **743–744**, 33–43.
21. Mangiarini,L., Sathasivam,K., Seller,M., Cozens,B., Harper,A., Hetherington,C., Lawton,M., Trottier,Y., Lehrach,H., Davies,S.W. *et al.* (1996) Exon 1 of the HD gene with an expanded CAG repeat is sufficient to cause a progressive neurological phenotype in transgenic mice. *Cell*, **87**, 493–506.
22. Biade,S., Sobol,R.W., Wilson,S.H. and Matsumoto,Y. (1998) Impairment of proliferating cell nuclear antigen-dependent apurinic/apyrimidinic site repair on linear DNA. *J. Biol. Chem.*, **273**, 898–902.
23. Macpherson,P., Barone,F., Maga,G., Mazzei,F., Karran,P. and Bignami,M. (2005) 8-oxoguanine incorporation into DNA repeats in vitro and mismatch recognition by MutSalpha. *Nucleic Acids Res.*, **33**, 5094–5105.
24. Beard,W.A. and Wilson,S.H. (1995) Purification and domain-mapping of mammalian DNA polymerase β. *Methods Enzymol.*, **262**, 98–107.
25. Turco,E., Ventura,I., Minoprio,A., Russo,M.T., Torreri,P., Degan,P., Molatore,S., Ranzani,G.N., Bignami,M. and Mazzei,F. (2013) Understanding the role of the Q338H MUTYH variant in oxidative damage repair. *Nucleic Acids Res.*, **41**, 4093–4103.
26. Pavlov,Y.I., Minnick,D.T., Izuta,S. and Kunkel,T.A. (1994) DNA replication fidelity with 8-oxodeoxyguanosine triphosphate. *Biochemistry*, **33**, 4695–4701.
27. Inoue,M., Kamiya,H., Fujikawa,K., Ootsuyama,Y., Murata-Kamiya,N., Osaki,T., Yasumoto,K. and Kasai,H. (1998) Induction of chromosomal gene mutations in Escherichia coli by direct incorporation of oxidatively damaged nucleotides. New evaluation method for mutagenesis by damaged DNA precursors in vivo. *J. Biol. Chem.*, **273**, 11069–11074.
28. Satou,K., Kasai,H., Masutani,C., Hanaoka,F., Harashima,H. and Kamiya,H. (2007) 2-Hydroxy-2′-deoxyadenosine 5′-triphosphate enhances A.T > C.G mutations caused by 8-hydroxy-2′-deoxyguanosine 5′-triphosphate by suppressing its degradation upon replication in a HeLa extract. *Biochemistry*, **46**, 6639–6646.
29. Beard,W.A., Batra,V.K. and Wilson,S.H. (2010) DNA polymerase structure-based insight on the mutagenic properties of 8-oxoguanine. *Mutat. Res.*, **703**, 18–23.
30. Batra,V.K., Beard,W.A., Hou,E.W., Pedersen,L.C., Prasad,R. and Wilson,S.H. (2010) Mutagenic conformation of 8-oxo-7, 8-dihydro-2′-dGTP in the confines of a DNA polymerase active site. *Nat. Struct. Mol. Biol.*, **17**, 889–890.
31. Freudenthal,B.D., Beard,W.A., Perera,L., Shock,D.D., Kim,T., Schlick,T. and Wilson,S.H. (2015) Uncovering the polymerase-induced cytotoxicty of an oxidized nucleotide. *Nature*, **517**, 635–639.
32. Miller,H., Prasad,R., Wilson,S.H., Johnson,F. and Grollman,A.P. (2000) 8-oxodGTP incorporation by DNA polymerase β is modified by active-site residue Asn279. *Biochemistry*, **39**, 1029–1033
33. Brown,J.A., Duym,W.W., Fowler,J.D. and Suo,Z. (2007) Single-turnover kinetic analysis of the mutagenic potential of 8-oxo-7, 8-dihydro-2′deoxyguanosine during gap-filling synthesis catalyzed by human DNA polymerases lambda and beta. *J. Mol. Biol.*, **367**, 1258–1269.
34. Kamiya,H., Maki,H. and Kasai,H. (2000). Two DNA polymerases of Escherichia coli display distinct misinsertion specificities for 2-hydroxy-dATP during DNA synthesis. *Biochemistry*, **39**, 9508–9513.
35. Shimizu,M., Gruz,P., Kamiya,H., Kim,S.R., Pisani,F.M., Masutani,C., Kanke,Y., Harashima,H., Hanaoka,F. and Nohmi,T. (2003) Erroneous incorporation of oxidized DNA precursors by Y-family DNA polymerases. *EMBO Rep.*, **4**, 269–273.

36. Tanaka,H., Arakawa,H., Yamaguchi,T., Shiraishi,K., Fukuda,S., Matsui,K., Takei,Y. and Nakamura,Y. (2000). A ribonucleotide reductase gene involved in a p53-dependent cell-cycle checkpoint for DNA damage. *Nature*, **404**, 42–49.

37. Pontarin,G., Ferraro,P., Bee,L., Reichard,P. and Bianchi,V. (2012) Mammalian ribonucleotide reductase subunit p53R2 is required for mitochondrial DNA replication and DNA repair in quiescent cells. *Proc. Natl. Acad. Sci. U.S.A.*, **109**, 13302–13307.

38. Håkansson,P., Hofer,A. and Thelander,L. (2006) Regulation of mammalian ribonucleotide reduction and dNTP pools after DNA damage and in resting cells. *J. Biol. Chem.*, **281**, 7834–7841.

39. van den Broek,W.J., Nelen,M.R., Wansink,D.G., Coerwinkel,M.M., te Riele,H., Groenen,P.J. and Wieringa,B. (2002) Somatic expansion behaviour of the $(CTG)_n$ repeat in myotonic dystrophy knock-in mice is differentially affected by Msh3 and Msh6 mismatch-repair proteins. *Hum. Mol. Genet.*, **11**, 191–198.

40. Møllersen,L., Rowe,A.D., Larsen,E., Rognes,T. and Klungland,A. (2010) Continuous and periodic expansion of CAG repeats in Huntington's disease R6/1 mice. *PLoS Genet.*, **6**, e1001242.

41. Møllersen,L., Rowe,A.D., Illuzzi,J.L., Hildrestrand,G.A., Gerhold,K.J., Tveterås,L., Bjølgerud,A., Wilson,D.M. 3rd, Bjørås,M. and Klungland,A. (2012) Neil1 is a genetic modifier of somatic and germline CAG trinucleotide repeat instability in R6/1 mice. *Hum. Mol. Genet.*, **21**, 4939–4947.

42. Lokanga,R.A., Senejani,A.G., Sweasy,J.B. and Usdin,K. (2015) Heterozygosity for a hypomorphic Polβ mutation reduces the expansion frequency in a mouse model of the Fragile X-related disorders. *PLoS Genet.*, **11**, e1005181.

43. Liu,Y. and Wilson,S.H. (2012) DNA base excision repair: a mechanism of trinucleotide repeat expansion. *Trends Biochem. Sci.*, **37**, 162–172.

44. Cilli,P., Minoprio,A., Bossa,C., Bignami,M. and Mazzei,F. (2015) Formation and repair of mismatches containing ribonucleotides and oxidized bases at repeated DNA sequences. *J. Biol. Chem.*, **290**, 26259–26269.

45. Owen,B.A., Yang,Z., Lai,M., Gajek,M., Badger,J.D., Hayes,J.J., Edelmann,W., Kucherlapati,R., Wilson,T.M. and McMurray,C.T. (2005) (CAG)(n)-hairpin DNA binds to Msh2-Msh3 and changes properties of mismatch recognition. *Nat. Struct. Mol. Biol.*, **12**, 663–670.

46. Pluciennik,A., Burdett,V., Baitinger,C., Iyer,R.R., Shi,K. and Modrich,P. (2013) Extrahelical (CAG)/(CTG) triplet repeat elements support proliferating cell nuclear antigen loading and MutLα endonuclease activation. *Proc. Natl. Acad. Sci. U.S.A.*, **110**, 12277–12282.

47. McMurray,C.T. (2008) Hijacking of the mismatch repair system to cause CAG expansion and cell death in neurodegenerative disease. *DNA Repair*, **7**, 1121–1134.

48. Mathews,C.K. (2006) DNA precursor metabolism and genomic stability. *FASEB J.*, **20**, 1300–1314.

49. Giuliano,P., De Cristofaro,T., Affaitati,A., Pizzulo,G.M., Feliciello,A., Criscuolo,C., De Michele,G., Filla,A., Avvedimento,E.V. and Varrone,S. (2003) DNA damage induced by polyglutamine-expanded proteins. *Hum. Mol. Genet.*, **12**, 2301–2309.

50. Pursell,Z.F., McDonald,J.T., Mathews,C.K. and Kunkel,T.A. (2008) Trace amounts of 8-oxo-dGTP in mitochondrial dNTP pools reduce DNA polymerase gamma replication fidelity. *Nucleic Acids Res.*, **36**, 2174–2181.

51. Sakumi,K., Furuichi,M., Tsuzuki,T., Kakuma,T., Kawabata,S., Maki,H. and Sekiguchi,M. (1993) Cloning and expression of cDNA for a human enzyme that hydrolyzes 8-oxo-dGTP, a mutagenic substrate for DNA synthesis. *J. Biol. Chem.*, **268**, 23524–23530.

52. Hayakawa,H., Hofer,A., Thelander,L., Kitajima,S., Cai,Y., Oshiro,S., Yakushiji,H., Nakabeppu,Y., Kuwano,M. and Sekiguchi,M. (1999) Metabolic fate of oxidized guanine ribonucleotides in mammalian cells. *Biochemistry*, **38**, 3610–3614.

53. Yamaguchi,H., Kajitani,K., Dan,Y., Furuichi,M., Ohno,M., Sakumi,K., Kang,D. and Nakabeppu,Y. (2006) MTH1, an oxidized purine nucleoside triphosphatase, protects the dopamine neurons from oxidative damage in nucleic acids caused by 1-methyl-4-phenyl-1, 2, 3, 6-tetrahydropyridine. *Cell Death Differ.*, **13**, 551–563.

54. Kajitani,K., Yamaguchi,H., Dan,Y., Furuichi,M., Kang,D. and Nakabeppu,Y. (2006) MTH1, an oxidized purine nucleoside triphosphatase, suppresses the accumulation of oxidative damage of nucleic acids in the hippocampal microglia during kainate-induced excitotoxicity. *J. Neuroscience*, **26**, 1688–1698.

55. Murakami,Y., Ikeda,Y., Yoshida,N., Notomi,S., Hisatomi,T., Oka,S., De Luca,G., Yonemitsu,Y., Bignami,M., Nakabeppu,Y. *et al.* (2012) MutT homolog-1 attenuates oxidative DNA damage and delays photoreceptor cell death in inherited retinal degeneration. *Am. J. Pathol.*, **181**, 1378–1386.

56. Haghdoost,S., Sjölander,L., Czene,S. and Harms-Ringdahl,M. (2006) The nucleotide pool is a significant target for oxidative stress. *Free Radic. Biol. Med.*, **41**, 620–626.

57. Molatore,S., Russo,M.T., D'Agostino,V.G., Barone,F., Matsumoto,Y., Albertini,A.M., Minoprio,A., Degan,P., Mazzei,F., Bignami,M. *et al.* (2010) MUTYH mutations associated with familial adenomatous polyposis: functional characterization by a mammalian cell-based assay. *Hum. Mutat.*, **31**, 159–166.

58. Sheng,Z., Oka,S., Tsuchimoto,D., Abolhassani,N., Nomaru,H., Sakumi,K., Yamada,H. and Nakabeppu,Y. (2012) 8-Oxoguanine causes neurodegeneration during MUTYH-mediated DNA base excision repair. *J. Clin. Invest.*, **122**, 4344–4361.